New architecture of organo electronic chalcones derivatives: Synthesis, crystal structures and optical properties

H. Belahlou, K. Waszkowska, A. Bouraiou, El-Eulmi Bendeif, S. Taboukhat, K. Bouchouit, B. Sahraoui

New architecture of organo electronic chalcones derivatives: Synthesis, Crystal Structures and Optical Properties

H. Belahlou[1, 2], K.Waszkowska[3], A. Bouraiou[1], El. Bendeif[4*], S. Taboukhat[3] and K. Bouchouit[5*] and B. Sahraoui[3]

[1]*Unité de Recherche de Chimie de 1'Environnement, et Moléculaire Structurale, CHEMS, Université Frères Mentouri, Constantine, 25000, Algérie*

[2]*Département de Chimie, Faculté des Sciences exactes et informatique, Université de Jijel, 18000 Jijel, Algérie*

[3]*Laboratory MOLTECH-Anjou, CNRS UMR 6200, University of Angers, 2 Bd Lavoisier, 49045 Angers CEDEX, France*

[4]Université de Lorraine, CNRS, CRM2, Nancy, France

[5]*Ecole Normal Supérieure de Constantine, Ville Universitaire, Constantine, Algérie*

*Correspondence e-mail: el-eulmi.bendeif@univ-lorraine.fr, karim.bouchouit@laposte.fr

Abstract

A series of four organics conjugate chalcone derivatives [**1**: (E)-2-(1-(3-oxo-1,3-diphenylprop-1-en-2-yl)pyridin-2(1H)-ylidene)malononitrile, **2**: (E)-2-(1-(3-oxo-3-phenyl-1-(p-tolyl)prop-1-en-2-yl)pyridin-2(1H)-ylidene)malononitrile, **3**: (E)-2-(1-(1-(4-methoxyphenyl)-3-oxo-3-phenylprop-1-en-2-yl)pyridin-2(1H)-ylidene)malononitrile, **4** : (E)-2-(1-(1-(4-chlorophenyl)-3-oxo-3-phenylprop-1-en-2-yl)pyridin-2(1H)-ylidene)malononitrile] were synthesized and structurally characterized by single-crystal X-ray diffraction, ^{1}H and ^{13}C NMR, FTIR and UV–Visible spectral analysis. The four studied compounds have the same molecular skeleton and the main difference corresponds to the substitution on the C13 carbon atom of the phenyl ring by a methyl, methoxy and chloride groups for **2**, **3** and **4** respectively. Third harmonic generation (THG) measurements have been performed on thin films at 1064 nm. To perform induced second harmonic generation measurements, the four molecular compounds were reoriented by using the corona poling technique on the films. These measurements highlight that compound **1** exhibits a significant NLO signature compared to the three other compounds. The effects of the substitution on the structural organizations and the optical properties is investigated and discussed.

Keywords: Chalcone, NLO, THG, SHG, X-ray diffraction, Crystal structure.

1. Introduction

Studies of the optical properties are in an increasing curve due to its potential applications in the area of optical data storage, communication, laser technology and image processing [1,2]. Organic and inorganic molecules with a high nonlinearity have been extensively investigated due to their applications in nonlinear optics including emission and absorption properties, laser applications, optic modulation, second and third harmonic generation, optical data storage, optical limiting and optical switching device [3,4]. Organic nonlinear optical materials, especially with delocalized electrons represent a large class of materials with high nonlinearity, fast quadratic and cubic NLO response and good optical damage threshold level [5-7].

A variety of organic electronics materials as chalcones derivatives has attracted chemists and physicists' attention mainly because of their ease of synthesis and its quadratic and cubic optical nonlinearities resulting from the significant delocalization of the π electrons of the chalcone system [8,9]. Chalcone derivatives molecules with a π conjugated system present an ideal NLO system because of his large charge transfer through substituent groups on the aromatic rings. The chemical structure of chalcones 1-4 consist of two aromatic rings connected by a propene unit which is formed by three carbon having a carbonyl group and one unsaturation. These compounds are obtained by condensation of an aromatic aldehyde and an aromatic ketone under acid catalysis or either base [10-13]. Due to their chemical structures which present a conjugated system that provides a large charge transfer axis with appropriate electron donor and electron acceptor substituent groups on the aromatic terminal rings. Furthermore, chalcones derivatives materials are the focus of considerable interest in pharmacological properties such as anti-inflammatory, antioxidative, anti-gout, anti-obesity, anti-histaminic, anti-protozoal, anti-spasmodic and hypnotic effects [14-18].

According to our previous works on the origin of the nonlinear response and the correlation between the chemical structure and the nonlinear properties [19-22]. Herein, we report on detailed the synthesis, characterization, optical and NLO results obtained from the study of four new organic electronic chalcones derivatives. The quadratic and cubic nonlinear optical properties of chalcones derivatives were evaluated.

2. Materials and methods

2.1. Synthesis and crystallization

All chemicals (reagents and solvents) used for the synthesis were purchased from Sigma Aldrich, and used without further purification.

Compound **1** was obtained from the reaction of pyridinium ylide with 2-benzylidenemalononitrile under ultrasound irradiation in the presence of triethylamine, in acetonitrile, at room temperature [23], while compounds **2, 3** and **4** were synthesized according to literature procedure [24]. 1-(phenylmethyl)-2-chloropyridinium bromides reacted with arylmethylenemalononitriles in the presence of a twofold excess of triethylamine as base to give 1-(1-benzoyl-2-arylvinyl)-2-dicyanomethylene-1,2-dihydropyridines **2, 3,** and **4**. The reactions occur under mild conditions.

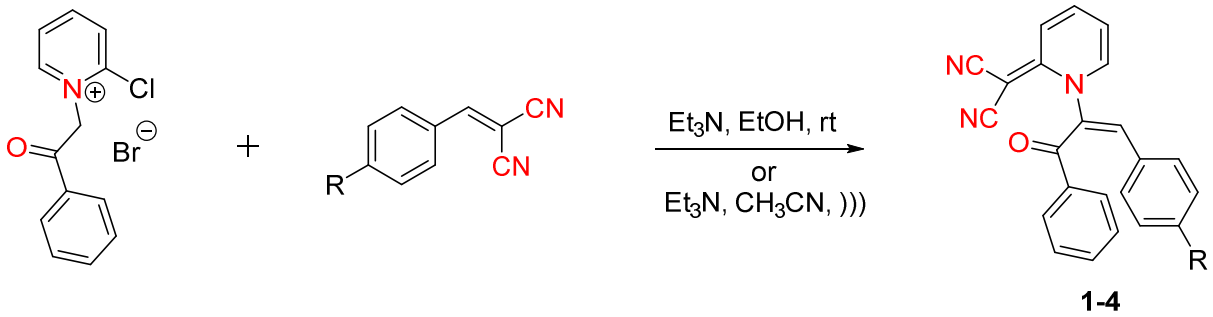

1-4

1: R = H (**72%**); **2:** R = Me (**78%**); **3**: R = OMe (**69%**); **4**: R = Cl (**84%**)

Scheme 1. Synthesis of compounds **1-4**

The molecular structures of the studied compounds have been confirmed by IR, UV-visible, and ^{1}H, ^{13}C NMR spectroscopy**.** The IR spectrum of compound **1** showed the presence of two C≡N groups by a two bands at 2160 and 2200 cm^{-1}, and showed one sharp band at 1655 cm^{-1} due to vibration of the carbonyl (C=O) group. The ^{1}H NMR spectrum of **1** indicated a triplet at 6.62 ppm. The olefinic proton is shifted to low field at 7.76 ppm, which confirmed conjugation of the double bond and the keto group. The aryl proton signals appeared at 7.92-7.09 ppm (13H, m)**.** The ^{13}C NMR of compound **1** showed a signal at 189.3 ppm, which was attributed to the carbonyl carbons. The others carbons appeared between 155.26 and 113.24 ppm.

2.2. Single-crystal X-ray diffraction measurements

The single crystal X-ray diffraction experiments were carried out at 100 K on a *SuperNova* dual wavelength microfocus diffractometer, equipped with a 135 mm Atlas CCD detector, using Mo-Kα radiation (λ=0.71093 Å) for **1** and **3** and Cu- Kα for **2** and **4** (λ=1.54184 Å). The

data collection, reduction, and analytical absorption corrections were performed with the *CrysAlis* program suite [25]. The crystals structures for the title compounds have been solved by direct methods and successive Fourier difference syntheses and refined by weighted full-matrix least squares method against F^2 using SHELX suite [26]. The corresponding structures are monoclinic and are described respectively in the $P2_1/c$ *(*for **1**), $P2_1/n$ (for **2** and **3**) and $C2/c$ (for **4**) spaces groups. Crystal data, data collection and structure refinement details are summarized in **Tab 1**. All non-hydrogen atoms are refined anisotropically. All H atoms were located in difference Fourier electron-density maps and were treated as riding on their parent atoms, with C-H = 0.950 Å, and Uiso(H) = 1.2x Uiso(C) for bond length distances and riding restraints, respectively. All calculations were carried out using the *WinGX* software package [27].

The cif-files of the studied compounds are available from the Cambridge Structural database under the numbers: CCDC 1995397-1995400**.**

Copies of the available material can be obtained, free of charge, on application to the Director, CCDC, 12 Union Road, Cambridge CB2 1EZ, UK, fax: +44 (0)1223 336033 or Email: deposit@ccdc.cam.ac.uk

Table 1. Crystal data, data collection and structure refinement for the four studied compounds.

Compound	**1**	**2**	**3**	**4**
Chemical formula	$C_{23}H_{15}N_3O$	$C_{24}H_{17}N_3O$	$C_{24}H_{17}N_3O_2$	$C_{23}H_{14}ClN_3O$
M	349.39	363.42	379.42	383.84
Crystal system	monoclinic	monoclinic	monoclinic	monoclinic
space group	P 2_1/c	P 2_1/n	P 2_1/n	C 2/c
a (Å)	8.7901(4)	8.5964(3)	8.5723(7)	24.3455(6)
b (Å)	16.2726(6)	18.1636(6)	18.8680(10)	8.7181(2)
c (Å)	12.8728(6)	12.7341(4)	12.9339(9)	17.8967(4)
β (°)	107.661(5)	102.391(3)	102.726(8)	101.177(2)
V (Å^3)	1754.51(14)	1942.01(11)	2040.6(3)	3726.47(15)
Z	4	4	4	8
T (K)	100	100	100	100
μ (mm^{-1})	0.083	0.616	0.080	1.962
Crystal size (mm)	0.29×0.26×0.15	0.23×0.12×0.11	0.20×0.18×0.11	0.23×0.21×0.14
Radiation type	Mo Kα	Cu Kα	Mo Kα	Cu Kα
Diffractometer	Agilent SuperNova CCD			
R_{int}	0.0537	0.0653	0.0523	0.0272
S	1.015	1.090	1.082	1.042
θ(°)	2.079; 35.266	4.308; 76.421	1.942; 33.11	3.701; 76.710
No. of measured reflections	54755	13127	26254	22401
No. of independent reflections	7534	4003	7106	3854
No. of observed [I > 2(I)] reflections	5670	3440	4893	3690
No. of parameters	248	257	266	257

2.3. Thin film preparation and optical absorption measurements

Thin films of the four studied compounds were prepared from DMSO (Dimethyl sulfoxide) solution of PMMA (Sigma-Aldrich, Mw=350,000 g mol^{-1}) with a concentration of 20 g. The mass concentration of the four the organic molecules in the PMMA matrix was 5 g. The thin films were deposited on cleaned glass substrates by using spin-coater (SCS G3) at 1200 rpm. To eliminate any remaining solvent obtained thin films were kept at 60° C for 4 hours in the oven. Thickness of prepared thin films was measured by using profilometer (Dektak 6M) and

the values are from around 145 to 583 nm. The obtained values of thickness and absorption peaks are given in **Tab. 2**.

Table 2: Thickness, absorption peaks and values of absorption coefficients for the four studied compounds.

Sample	Thickness [nm]	λ_{abs} [nm]	α [10^3 cm^{-1}]	
			355 nm	532 nm
1	(145.92 ± 1.21)	391	6.78	0.31
2	(455.26 ± 6.74)	332; 389	2.99	0.24
3	(543.49 ± 10.71)	338; 389	2.39	0.03
4	(582.50 ± 2.72)	346	9.05	0.34

2.4. Nonlinear optical measurements

The second harmonic (SHG) and third harmonic (THG) measurements were carried out by using a well-known Maker fringe setup [28, 29] which is schematically presented on Fig. 1. Intensities of generated harmonics as a function of incident angle were measured during rotation of samples from -75° to +75° in horizontal and vertical polarizations (S-, and P-, respectively). As a source of light, Nd:YAG laser (Ekspla, PL2250) generating wavelength 1064 nm, pulse duartion 30 ps, energy aroun 60 μJ and frequency of 10 Hz has been used. Moreover, no restriction of polarized beam has been noticed during THG experiment.

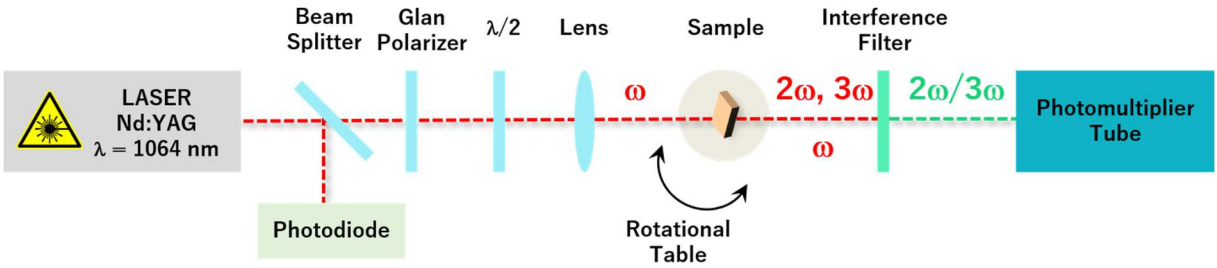

Figure 1. SHG and THG experimental setup via Maker fringe technique.

3. Results and discussion

3.1. Structural commentary

The crystallographic analysis of the studied compounds confirm the results of the spectroscopic measurements. The molecular structures of the four compounds are shown in **Figure 2**.

All compounds crystallize in monoclinic centrosymmetric space groups. Given the fact that the four studied compounds have the same molecular skeleton and the main difference corresponds to the substitution on the C13 carbon atom of the phenyl ring by a methyl, methoxy and chloride groups for **2**, **3**and **4** respectively. We therefore describe below only the structural properties of the first compound, namely ((E)-2-(1-(3-oxo-1,3-diphenylprop-1-en-2-yl)pyridin-2(1H)-ylidene)malononitrile: **1**) and we will discuss the effects of substitution on the structural organizations of the other three compounds (**2**, **3** and **4**).

Compound **1** crystallized in the $P2_1/c$ space group of the monoclinic crystal system. Its asymmetric unit is composed of three fragments: one (pyridin-2-ylidene) malononitrile moiety, one benzoyl group and one phenyl ring. The (pyridin-2-ylidene) malononitrile group is connected to chalcone unit. This unit adopts an **E** conformation through the propene moiety (C1-C8-C9) that bridges the benzoyl ant the phenyl aromatic groups (**Fig 2**). One notes, that these aromatic groups are rotated to each other so that their mean planes form an angle of 60.20(2) degrees. It is very important to point out that that this angle is very different in the other three compounds (35.36(3) ° for **2**, (38.36(3) ° for **3** and 67.47(3) ° for **4**). This significant difference is very probably correlated on the one hand to the substitution at the phenyl ring level (C13) and on the other hand to the molecular environment of each compound, *i.e*. in other words, intermolecular interactions.

The phenyl ring is almost perfectly planar however, the benzoyl group shows a non-planar structure and we observe a significant displacement of O1 atom (0.850(2) Å) from the ring mean plan. This deviation from planarity has also observed in the three other crystals structures. Indeed, the displacements observed for the oxygen atom O1 are of 0.878(3) Å, 0.810(2) Å and 0.704(3) Å for **2**, **3** and **4** respectively.

In the propene bridge, the C9—C10, C1—C8 and C1—C2 bond lengths of 1.462(1) Å, 1.490(1) Å and 1.488(1) Å, respectively, clearly indicate the σ bond type of this fragment. While the C8-C9 and C1-O1 bond lengths of 1.343(1) Å and 1.222(1) Å, respectively, confirm the π character of these bonds. The C8—C9—C10 and C2—C1—C8 bond angles are

of 131.64(9) and 119.91(8) °, respectively, and thus confirm the sp2 hybridization of C1, C8 and C9 carbon atoms.

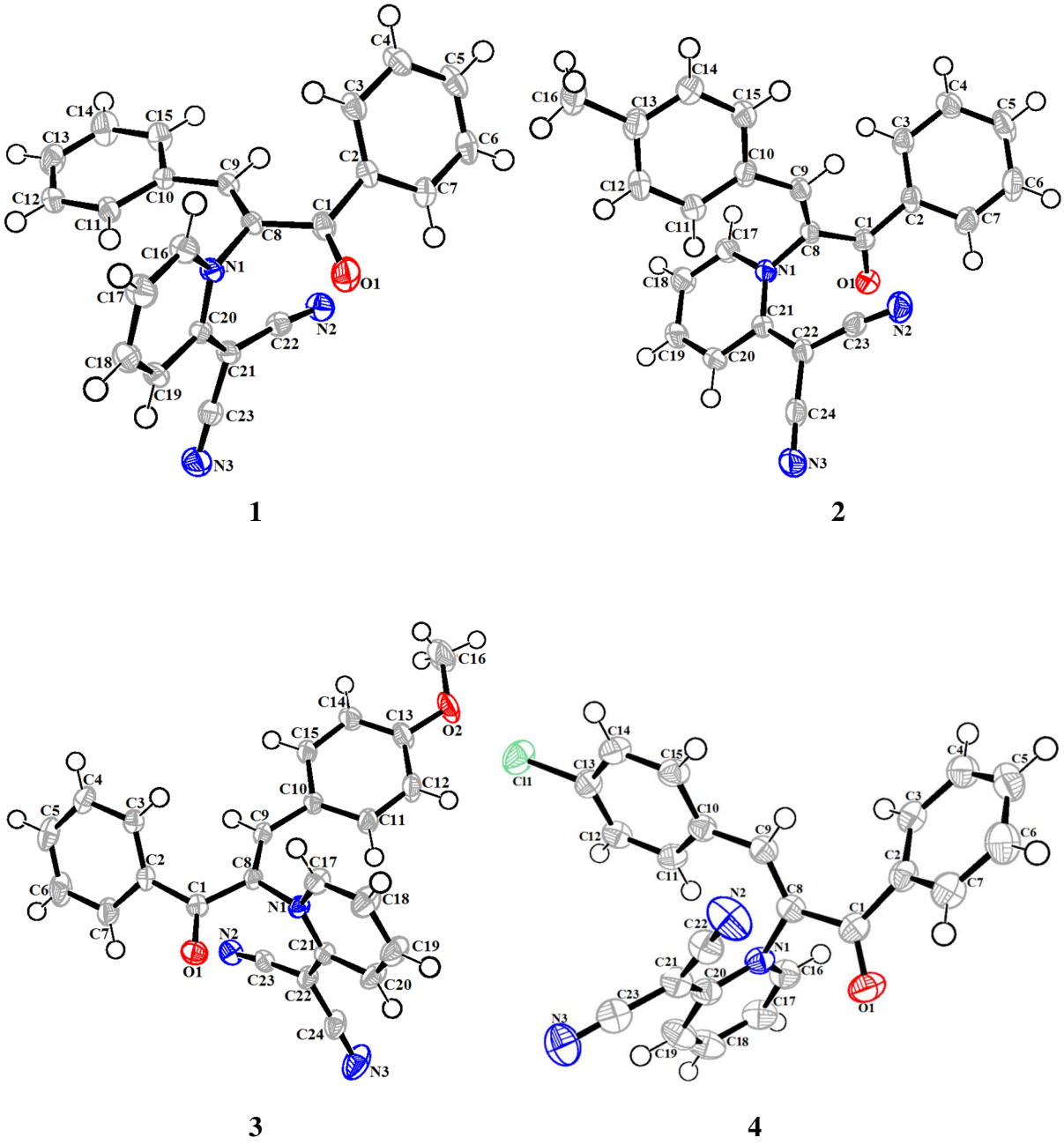

Figure 2. ORTEP view of the asymmetric units of the four title compounds (**1-4**) with atom-numbering scheme. Hydrogen atoms labels have been omitted for clarity. Displacement ellipsoids are drawn at the 50% probability level.

The C8=C9 double bond adopts an *E* conformation [C10—C9—C8—C1 torsion angle = 176.42(9) °]. The conformation of the different fragments of compound **1** can be defined by four torsion angles. The torsion angles between the phenyl ring and the olefinic double bond

(C11—C10—C9—C8, **τ1**), between the olefinic double bond and the carbonyl group (C9—C8—C1—O1, **τ2**)**,** between the olefinic double bond and the pyridine fragment (C9—C8—N1—C20, **τ3**) and between the carbonyl group and the phenyl ring (C8—C1—C2—C3, **τ4**). The torsion angles **τ1** and **τ2** are respectively of 3.04(2) ° and 15.62(1) °, indicating that the phenyl ring and the enone bridge are coplanar. In contrast, the pyridine fragment is nearly perpendicular to the attached phenyl ring, as shown by the angle **τ3** of 86.99(1) °. Moreover, the **τ4** torsion angle of 134.69(9) ° clearly indicates that the carbonyl group is deviated from the phenyl fragment.

The three-dimensional crystal packings of the studied compounds are built of organic molecular species interconnected by weak C—H…N and C-H…O hydrogen bonds and C-H…Cl interactions (for compound **4**). The three-dimensional networks are also characterized by the presence of weak C-H···C and C—H…π interactions intermolecular interactions.

In the four compounds, the malononitrile N2 atom is involved in the hydrogen bonding networks and acts as a bifurcated acceptor. It is noteworthy that the behavior the malononitrile N3 is different. Indeed, in compound **1**, similarly to N2, N3 acts as a bifurcated acceptor, however, it participates in only one C—H…N hydrogen bond in compound **2**. For compounds **3** and **4**, the N3 is not involved in the network of intermolecular interactions. It is worth noting the like-π… π stacking observed between the pyridine ring and the benzoyl group in compound **1**. This arrangement is generated by the C-H…O interactions involving the carbonyl group and a neighboring benzoyl group. One notes that in addition to the molecular structure of compound **1**, its intermolecular interactions network is more favorable for efficient charge transfer compared to the other three compounds.

3.2. UV-visible spectra

The absorption spectra of the title compounds, which were dissolved in acetonitrile (ACN) and diluted into PMMA matrix, are presented in Fig. 3. The maxima of absorption bands are located at 300 and 390 nm in solutions and at 340 and 390 nm in films which are assigned to $\pi \rightarrow \pi^*$ and $\delta \rightarrow \delta^*$ transitions respectively. Also we can notice that all these compounds present high transparency at the wavelength of more than 500 nm. Moreover, according to absorption spectra (Fig. 2) one observes that at wavelengths corresponding to the generated third harmonics (THG), the absorbance is not negligible. It determines that the absorption process affects the generated THG response. It is therefore mandatory to take into account the

absorption coefficient in NLO calculations. The calculated values of absorption coefficients for 532 nm (SHG) and 355 nm (THG) are given in Tab. 1.

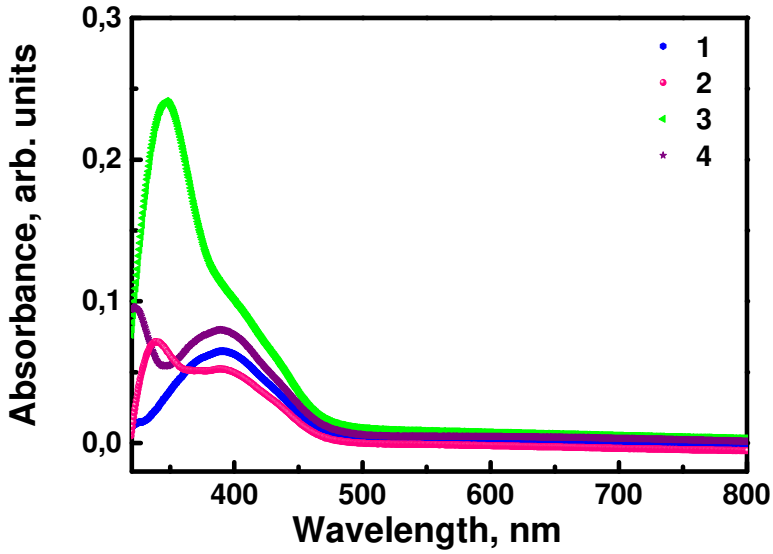

Figure 3: Absorption spectra of the four studied compounds embedded in PMMA thin films.

3.3. SHG Results

In the case of SHG response, the dependence of polarization of fundamental laser beam was noticed. We observed a higher response for p-polarization, it means that the generated second harmonic is polarized in a perpendicular direction to the thin films. The highest response was noticed for the compound **1**. From the crystallographic data reported in table 1, all these compounds crystallize in centrosymmetric groups. However, it is well known that the SHG response is impossible in centrosymmetric groups; we therefore have proceeded to the reorientation of the molecules in the thin films by using the corona poling technique [30]. This method allows breaking the centrosymmetric alignment of the films and induce the SHG response of the studied compounds. As a reference material for SHG measurements, we used Y-cut quartz glass with 1mm thickness. Fig. 4 shows the obtained SHG intensities as a function of incident angle for the four compounds.

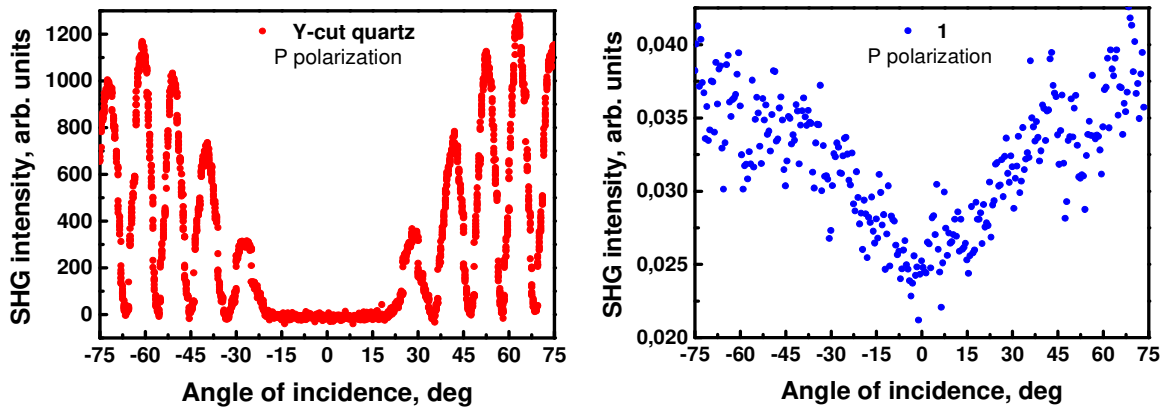

Figure 4: SHG response of Y-cut quartz glass and compound 1 thin film in P-polarization.

The second-order nonlinear optical susceptibility was calculated by using the Lee model [31]:

$$\chi^{(2)} = \chi^{(2)}_{Quartz}\left(\frac{2}{\pi}\right)\left(\frac{L^{coh}_{Quartz}}{d}\right)\left(\frac{\frac{\alpha d}{2}}{1-exp\left(-\frac{\alpha d}{2}\right)}\right)\sqrt{\frac{I^{2\omega}}{I^{2\omega}_{Quartz}}}$$

where: $\chi^{(2)}_{Quartz} = 1 \cdot 10^{-12} m \cdot V^{-1}$[32], $L^{coh}_{Quartz} = 21\,\mu m$ is the coherence length of reference material, , d – sample thickness, α - linear absorption coefficient, $I^{2\omega}$ and $I^{2\omega}_{Quartz}$ are SHG intensities of thin film and reference material, respectively. The calculated susceptibilities are given in tab. 3.

From table 3, the SHG response for compounds **1-4** for p-p input-output polarization configuration was found higher than for s-p method. This difference is due to the values of tensor elements $\chi^{(2)}$ responsible for the corresponding scheme of the experiment – $\chi^{(2)}_{zzz}$ and $\chi^{(2)}_{zxx}$. For molecular systems the theoretically predicted ratio $\chi^{(2)}_{zzz}/\chi^{(2)}_{zxx}=3$ [33]. The higher quadratic NLO response has been obtained for compound **1**, where the electron-donating substitution on the carbon C13 position is missing. The important decrease of second-order nonlinear optical susceptibility $\chi^{(2)}$ for s-p polarization of compounds **2**, **3** and **4** comparing to **1** is due to the presence of different donor groups and hence less charge transfer in this compounds. Moreover, the electron-donating Cl, OCH_3 and CH_3 groups reduce the conjugated length and consequently inhibit efficient π electron delocalization and charge transfer within these compounds. All of these factors influence the quadratic NLO response.

3.4. THG Results

To extract and evaluated the third-order NLO susceptibility of compounds 1-4 thin films, were calculated by using the Kubodera-Kobayashi model [34]:

$$\chi^{(3)} = \chi^{(3)}_{Silica}\left(\frac{2}{\pi}\right)\left(\frac{L^{coh}_{Silica}}{d}\right)\left(\frac{\frac{\alpha d}{2}}{1-exp\left(-\frac{\alpha d}{2}\right)}\right)\sqrt{\frac{I^{3\omega}}{I^{3\omega}_{Silica}}}$$

where: $\chi^{(3)}_{Silica} = 2 \cdot 10^{-22} m^2 \cdot V^{-2}$[35], $L^{coh}_{Silica} = 6{,}7\mu m$ is the coherence length of reference material, α - linear absorption coefficient, d – sample thickness and $I^{3\omega}$ and $I^{3\omega}_{Silica}$ are THG intensities of thin film and reference material, respectively.

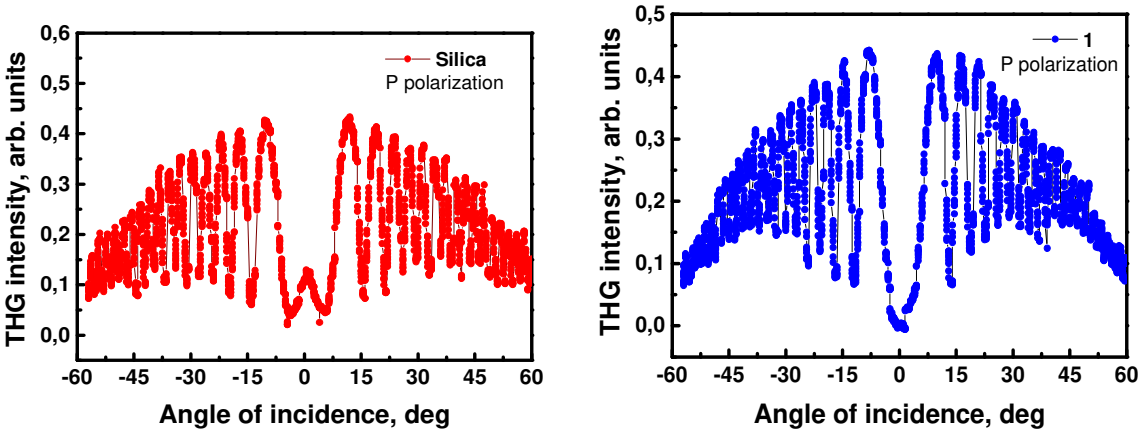

Figure 5: THG response of silica glass and compound **1** thin film in p-polarization.

Fig. 5 present THG intensities as a function of incident angle that is collected for compound **1**. The $\chi^{(3)}$ THG susceptibilities values for compounds **1-4** were estimated and evaluated by comparing the THG signal with that SiO_2 glass material. As a reference material in THG measurements was used silica glass with thickness 1 mm. In our calculations we used formula 2. The calculated values of third order NLO susceptibility $\chi^{(3)}$ are given in tab. 3. The obtained values of cubic susceptibility $\chi^{(3)}$ of compounds **1-4** thin films at a measurement wavelength of 1064 nm have been estimated at $1{,}5 \cdot 10^{-21}$ [m^2V^{-2}] and $6 \cdot 10^{-21}$ [m^2V^{-2}] (Table 3). These values are one order of magnitude larger than susceptibility $\chi^{(3)}$ value of silica, which is the reference material for THG measurements. Also, we can observe from Table 3 that the cubic susceptibility $\chi^{(3)}$ THG of molecule **1** is more important than $\chi^{(3)}$ of compound **2,3** and **4**. Moreover, the cubic and the quadratic for polarization s-p nonlinearity is inversely proportional.

Table 3: Calculated second- and third-order nonlinear optical susceptibility.

Sample	$\chi^{(2)}$ [pmV^{-1}]		$\chi^{(3)}$ [10^{-22} m^{2}V^{-2}]
	s-p	p-p	p-p
Quartz	1.00		-
Silica	-		2.00
1	**0.545**	**0.572**	**60.89**
2	0.175	0.163	19.97
3	0.086	0.132	17.35
4	0.141	0.242	14.35

Conclusion

In summary, we have presented in this work the synthesis, structural analysis and nonlinear optical (NLO) properties of four novel organo electronics chalcone derivatives. The Single-crystal analysis revealed that the four molecular structures adopt an E conformation and can be described in monoclinic centrosymmetric space groups. The stabilization of the crystal structures of the four compounds is provided by weak C-H...N, C-H...O and C-H...O hydrogen bonds and C—H…π interactions. The third order NLO susceptibility were evaluated on thin films by using third harmonic generation (THG) measurements at 1064 nm. For the induced second harmonic generation measurements, we have reversed the symmetry by using the corona poling technique. We found that the quadratic nonlinear responses decrease proportionally with the influence of the electron-donating groups Cl < OCH_3 < CH_3. We also observed a higher response for p-polarization, it means that generated second harmonic is polarized in a perpendicular direction to the thin films. The highest response of both, SHG and THG was observed for compound **1**. This behavior may be explained by the molecular structure of **1** and more efficient charge transfer generated by a favorable three-dimensional intermolecular interactions network.

Acknowledgements

We are grateful for measurement time on the X-ray diffraction platform PMD²X of the Institute Jean Barriol, Université de Lorraine.

References

[1] Ralph, T. C.; Boyd, R. W. Better Computing with Photons. Science 2007, 318, 1251-1252.

[2] H.S. Nalwa, S. Miyata, Nonlinear Optics of Organic Molecules and Polymers, CRC press, 1996.

[3] Kajzar, F.; Swalen, J. D. Eds., Organic Thin Films for Waveguiding Nonlinear Optics; Gordon and Breach, Amsterdam, 1996.

[4] R.W. Boyd, Nonlinear Optics, Academic Press, 2003.

[5] H. El Ouazzani, K. Iliopoulos, M. Pranaitis, O. Krupka, V. Smokal, A. Kolendo and B. Sahraoui, J. Phys. Chem. B, 2011, 115, 1944–1949.

[6] M. Maaza, N. Mongwaketsi, M. Genene, G. Hailu, G. Garab, B. Sahraoui and D. Hamidi, J. Porphyrins Phthalocyanines, 2012, 16, 985–995.

[7] I. Fuks-Janczarek, J. Luc, B. Sahraoui, F. Dumur, P. Hudhomme, J. Berdowski and I. V. Kityk, J. Phys. Chem. B, 2005, 109, 10179–10183.

[8] D'silva, E. D., Podagatlapalli, G. K., Rao, S. V., Rao, D. N. & Dharmaprakash, S. M. (2011). Cryst. Growth Des. 11, 5326–5369.

[9] Wu, W., Liu, Y. & Zhu, D. (2010). Chem. Soc. Rev. 39, 1489–1502.

[10] Chimenti, F., Fioravanti, R., Bolasco, A., Chimenti, P., Secci, D., Rossi, F., Yanez, M., Orallo, F., Ortuso, F., Alcaro, S., Cirilli, R., Ferretti, R. & Sanna, M. L. (2010). Bioorg. Med. Chem. 18, 1273–1279.

[11] Elarfi, M. J. & Al-Difar, H. A. (2012). Sci. Rev. Chem. Commun. 2, 103–107.

[12] Ghosh, R. & Das, A. (2014). World J. Pharm. Pharma. Sci. 3, 578–595.

[13] Hamada, N. M. & Sharshira, E. M. (2011). Molecules, 16, 2304–2312.

[14] Robinson, S. J., Petzer, J. P., Petzer, A., Bergh, J. J. & Lourens, A. C. U. (2013). Bioorg. Med. Chem. Lett. 23, 4985–4989.

[15] Sharma, P., Kumar, S., Ali, F., Anthal, S., Gupta, V., Khan, I., Singh, S., Sangwan, P., Suri, K., Gupta, B., Gupta, D., Dutt, P., Vishwakarma, R. & Satti, N. (2013). Med. Chem. Res. 22, 3969–3983.

[16] Zheng, C. J., Jiang, S.-M., Chen, Z. H., Ye, B.-J. & Piao, H. R. (2011). Arch. Pharm. Pharm. Med. Chem. 344, 689–695.

[17] Yamamoto, T., Yoshimura, M., Yamaguchi, F., Kouchi, T., Tsuji, R., Saito, M., Obata, A. & Kikuchi, M. (2004). Biosci. Biotechnol. Biochem. 68, 1706–1711.

[18] Israf, D. A., Khaizurin, T. A., Syahida, A., Lajis, N. H. & Khozirah, S. (2007). Mol. Immunol. 44, 673–679.

[19] K. Bouchouit, Z. Essaidi, S. Abed, A. Migalska-Zalas, B. Derkowska, N. Benalicherif, M. Mihaly, A. Meghea, B. Sahraoui, Chem. Phys. Lett. 455 (2008) 270

[20] S. Arroudj, M. Bouchouit, K. Bouchouit, A. Bouraiou, L. Messaadia, B. Kulyk, V. Figa, S. Bouacida, Z. Sofani, S. Taboukhat, Opt. Mater. 56, 116 (2016)

[21] M. Bouchouit, Y. Elkouari, L. Messaadia, A. Bouraiou, S. Arroudj, S. Bouacida, S. Taboukhat, K. Bouchouit, Opt. Quant. Electron. 48 (2016) 178.

[22] K. Bouchouit, E. Bendeif, H. E. Ouazzani], S. Dahaoui, C. Lecomte,N. Benali-cherif, B. Sahraoui, Correlation between structural studiesand third order nlo properties of selected new quinolinium semi-organiccompounds, Chem. Phys. 375 (2010) pp 1 – 7.

[23] Mehdi Abaszadeh and Mohammad Seifi, Org. Biomol. Chem., 12, 7859, 2014.

[24] G. E. Khoroshilov,Chemistry of Heterocyclic Compounds, Vol. 37, No. 9, 2001.

[25] Rigaku Oxford Diffraction. 2018. CrysAlis CCD and CrysAlis RED. (*Versions 1.171.39.46*).

[26] Sheldrick, G.M. Acta Cryst. **2015**, C71, 3–8.

[27] Farrugia, L. J. J. Appl. Cryst. **1999**, 32, 837–838.

[28] B. Sahraoui, J. Luc, et al. J. Opt. A, Pure Appl. Opt. 11, 2009.

[29] A. Zawadzka, K. Waszkowska, et al. Dyes and Pigments, Volume 157, Pages 151-162, 2018.

[30] Z. Essaidi, O. Krupka, et al. Opt. Mater. 35, 3, Pages 576-581, 2013

[31] G. J. Lee, et. al. J. Kor. Phys. Soc., 39(5), 912-915, 2001.

[32] S.K. Kurtz, J. Jerphagnon, M.M. Choy, Landolt-Boernstein New Ser. 11 (1979) 671.

[33] P.N. Prasad, D.J. Williams, Introduction to Nonlinear Optical Effects in Molecules & Polymers, Wiley, New York (1991)

[34] K. Kubodera, H. Kobayashi, Mol. Crys. Liq. Crys. Inc. NLO, 182:1, 103-113, 1990.

[35] F. Kajzar, Y. Okada-Shudo, C. Merrit, Z. Kafafi, Synth. Met. 117, 2001.